



## Synthesis of hexagonal AlN microbelts at low temperature

H.L. Wang<sup>a,\*</sup>, H.M. Lv<sup>b</sup>, G.D. Chen<sup>a</sup>, H.G. Ye<sup>a</sup>

<sup>a</sup> School of Science, Xi'an Jiaotong University, Xi'an, Shaanxi 710049, People's Republic of China

<sup>b</sup> Department of Applied physics, Xi'an University of Technology, Xi'an, Shaanxi 710048, People's Republic of China

### ARTICLE INFO

#### Article history:

Received 29 July 2008

Received in revised form 13 October 2008

Accepted 20 October 2008

Available online 4 December 2008

#### Keywords:

*h*-AlN

Microbelts

Photoluminescence spectrum

Growth mechanism

### ABSTRACT

Pure hexagonal aluminum nitride microbelts have been successfully synthesized by directly reacting  $\text{AlCl}_3$  with  $\text{NaN}_3$  at low temperature under the condition of non-solvent system. The reaction product (gray-white powder) is characterized by High Resolution Transmission Electron Microscope (HRTEM), the result reveals that the product has a long curling belts morphology with the length of several micrometers. The results of both electron diffraction (ED) and X-ray diffraction (XRD) indicate that the AlN microbelts have a pure hexagonal monocrystalline structure with slight curling. A room temperature photoluminescence spectrum (PL) of the synthesized sample shows an emission peak at 422 nm. The growth mechanism and photoluminescence spectrum of AlN microbelts are discussed.

© 2008 Elsevier B.V. All rights reserved.

### 1. Introduction

As one of the III nitrides, AlN possesses a direct band gap of 6.2 eV [1], which is close to that of an insulator. Its resistivity ( $>10^{11} \Omega \text{ m}$ ) is very high, while its dielectric constant (8.6) is very low. Due to these properties, AlN is ideal for use of electronic substrate material and integrated circuit packaging material [2]. It has high thermal conductivity ( $320 \text{ W m}^{-1} \text{ K}^{-1}$ ) [3], which is three times as high as that of  $\text{Al}_2\text{O}_3$  which is of the highest value among the ceramic materials ever found, and it has low coefficient of thermal expansion ( $4.3 \times 10^{-6} \text{ K}^{-1}$ ), so AlN can be used to solve the problem of thermal matching between the substrate and the semiconductor, and the cooling problem of high power electronic devices caused by the integration and micromation [4]. AlN can form ternary alloys AlGaN and AlInN with Ga and In, and their band gap can be controlled from 0.7 eV to 6.2 eV, so they are very suitable for the fabrication of optical detectors covering the range from infrared to UV. AlGaN and AlInN can also be used in pressure sensors, thermal radiation detectors, field effect transistors [5,6] and catalysts in chemical reactions [7]. Due to its excellent optical and acoustic properties, AlN can also be used for surface acoustic wave devices as well [8]. Recently, though randomly oriented AlN nanowires [9–11], nanotubes [12] and well-aligned nanowires [13] have been fabricated, and aligned AlN have been synthesized using anodic alumina membrane templates [14], fabrication of high-quality and

well-aligned AlN nanowire arrays are still difficult compared to the similar system of GaN nanowire arrays [15]. AlN nanowires, nanotubes and microbelts are promising materials in future application.

AlN is traditionally synthesized by ion beam evaporation [7] and direct current electric arcing. In these procedures, aluminum is compelled to separate from its precursor under extreme conditions, and then reacts with ammonia or nitrogen [6,16]. Another approach to synthesize AlN is to separate carbon from hydrocarbon, and then let it react with  $\text{Al}_2\text{O}_3$  in ammonia or nitrogen environment at high temperature ( $>1600^\circ\text{C}$ ) for several hours [17]. Under high pressure ( $>1000 \text{ atm}$ ) and high temperature ( $>1900^\circ\text{C}$ ), AlN is also successfully synthesized by reacting aluminum powder with atomic nitrogen or  $\text{NaN}_3$  [18]. However, the equipments used in the above methods are expensive, and the experimental condition is relatively severe and difficult to achieve in most laboratories.

### 2. Experimental details

AlN microbelts are synthesized in a stainless-steel autoclave in the absence of solvent or any catalyst. Anhydrous  $\text{AlCl}_3$  and  $\text{NaN}_3$  are put into the autoclave under a dry and pure nitrogen environment, and then the autoclave is put into a furnace to heat. The reaction temperature is controlled at  $450^\circ\text{C}$  and kept for 24 h, then the autoclave is taken out of the furnace and cooled naturally down to room temperature. The by-product NaCl and other impurities are removed by de-ionized water, and then the product is dried. The gray-white powder is the final product in the experiments. The product is examined by High Resolution Transmission Electron Microscope (HRTEM, JEOL, JEM-3010), electron diffraction (ED, JEOL, JEM-3010), X-ray diffraction (XRD, JEOL, XRD-7000S, Cu:  $1.5405620 \text{ \AA}$ ), and photoluminescence spectra (PL, Ocean Optics, HR2000), respectively.

\* Corresponding author. Tel.: +86 2982668503; fax: +86 2982668000.  
E-mail address: [wang.h.l@stu.xjtu.edu.cn](mailto:wang.h.l@stu.xjtu.edu.cn) (H.L. Wang).

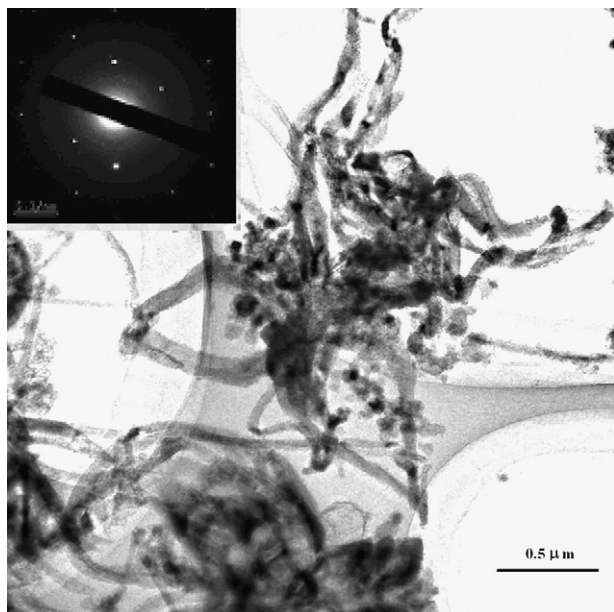


Fig. 1. HRTEM pictures of AlN microbelts. The inset figure is the ED pattern of the microbelts, which indicated that the microbelts are monocrystalline.

### 3. Results and discussion

The product is examined by HRTEM (see Fig. 1), the photo shows that most of the sample exhibit the morphology of long curling belts without branches. The surface of the belts is smooth and relatively uniform without any deposit. The length of most of the microbelts is several micrometers. Besides these microbelts, there are some long straight nanowires, as indicated by 'A' in Fig. 2. The diameter of the nanowires ranges from 40 nm to 60 nm, and their length is also several micrometers. The inset in Fig. 1 is the ED pattern of the AlN microbelts, which shows that the microbelts are monocrystalline growing along the [0001] direction. The product is examined by XRD, and the result is shown in Fig. 3. The sample is ascertained to be *h*-AlN with lattice constants of

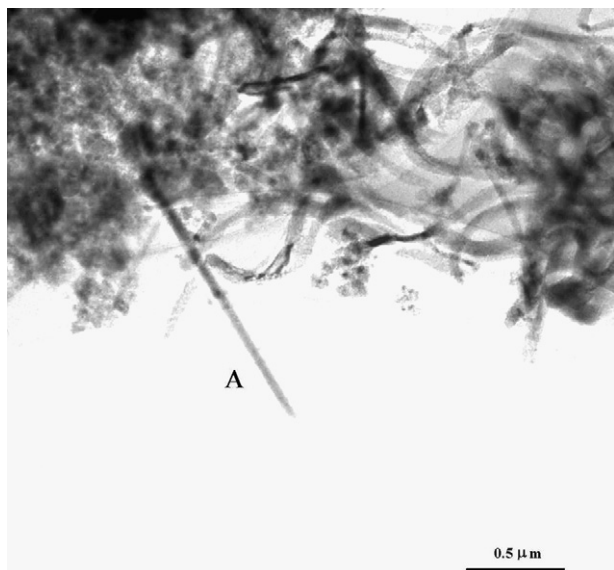


Fig. 2. HRTEM pictures of AlN microbelts with accompanying long straight-wire morphology nanowires, as indicated by 'A'.

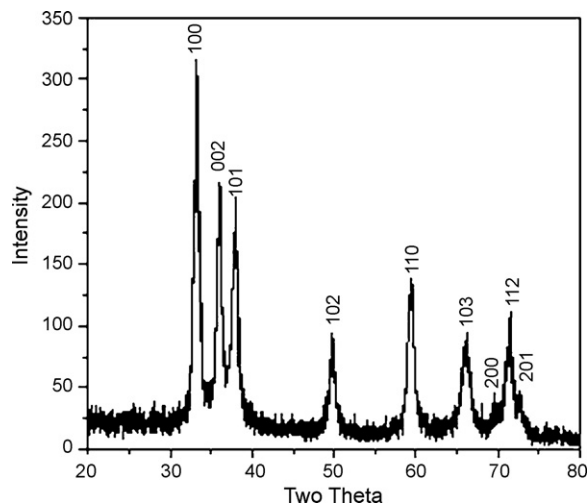


Fig. 3. XRD pattern of AlN: the calibrated peaks indicate that the material has a hexagonal monocrystalline structure.

$a = 3.109 \text{ \AA}$  and  $c = 4.979 \text{ \AA}$  compared with the standard XRD patterns.

The above method to synthesize AlN microbelts is based on the metathetical reaction of  $\text{AlCl}_3$  and  $\text{NaN}_3$ . In the experiments, the reaction temperature is controlled at  $450^\circ\text{C}$ , which is higher than the sublimation temperature of  $\text{AlCl}_3$  ( $177.8^\circ\text{C}$ ) and the chemical decomposition temperature of  $\text{NaN}_3$  ( $330^\circ\text{C}$ ) [19–21]. Because the binding energies of AlN and NaCl are higher than those of  $\text{AlCl}_3$  and  $\text{NaN}_3$ , AlN and NaCl are more stable than  $\text{AlCl}_3$  and  $\text{NaN}_3$ . Therefore, the reaction in experiments must tend to produce AlN and NaCl. NaCl is relatively stable and does not participate in other reaction again, it will crystallize to form micro-crystals during the cooling process and then is filtered out as the by-product.

With regard to the growth mechanism of *h*-AlN, there are several hypotheses, such as "vapor–solid" [22], "liquid–solid", "vapor–liquid–solid" [23]. The AlN is very possibly synthesized via "vapor–solid" mechanism in the experiments. Because the NaCl melting point ( $801^\circ\text{C}$ ) is much higher than the reaction temperature ( $450^\circ\text{C}$ ), the liquidization is impossible. When the reaction temperature reaches up to  $330^\circ\text{C}$ ,  $\text{AlCl}_3$  will sublime before  $\text{NaN}_3$  starts to decompose, meanwhile the extricated neutral nitride and sodium atoms will generate, so AlN is likely to be synthesized via "vapor–solid" mechanism. When the reaction temperature reaches the setting value of  $450^\circ\text{C}$ , the above reaction should end at a certain time. The produced AlN, NaCl and other little residual matter exist as micro-crystals or molecular clusters, and spread in the high pressure environment which consists of  $\text{N}_2$  and N during the latter 20 h. The temperature is kept at  $450^\circ\text{C}$  and these AlN molecular clusters combine to form crystal nuclei or molecular chains, and these molecular clusters grow up to microbelts abiding by the preferential selection mechanism. Because the orientation of the nuclei is stochastic, the orientation of the microbelts is also stochastic. Meanwhile the molecular chains combine with each other and condense to form whiskers and zones. Whisker/whisker, zone/zone, and whisker/zone have mutual interactions and combine to form thin films with large areas under the high temperature and high pressure. Some films become curled under internal stress.

Fig. 4 shows the photoluminescence spectra of the synthesized sample at room temperature, which has an emission peak at  $422 \text{ nm}$ . In the experiment, the photon energy of the  $355 \text{ nm}$  laser (exciting light) is below the band gap ( $6.2 \text{ eV}$ ) of AlN, so the

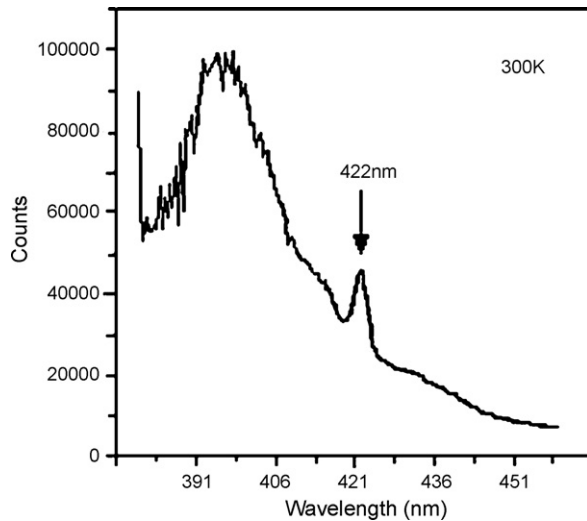


Fig. 4. PL spectrum of AlN at room temperature.

purple emission cannot be excited in the experiment. The observed emission peak may be caused by deep level defects, such as oxygen impurities, aluminum vacancy and antisite defects of N and Al [24–27].

#### 4. Conclusions

Hexagonal monocrystalline *h*-AlN microbelts have been successfully synthesized through direct reaction of anhydrous AlCl<sub>3</sub> and NaN<sub>3</sub> at low temperature of 450 °C for about 24 h. This is a simple method and the first time to synthesize hexagonal monocrystalline AlN microbelts since nanometer AlN whiskers were synthesized by Wu et al. in 2004 [28]. It is more important that the growth mechanism of AlN nanowires and microbelts is probably “vapor–solid” hypotheses. The PL spectra are also discussed, and the emission peak may be caused by oxygen impurities, aluminum vacancy and antisite defects of N and Al.

#### Acknowledgments

This work was supported by the National Natural Science Foundation of China (Grant No. 10474078). We are grateful to Prof. L.Q. Huang and Dr. G.J. Yan for useful discussions.

#### References

- [1] Y. Goldberg, M.E. Levinshtein, S.L. Rumyantsev, M.S. Sur, *Properties of Advanced Semiconductor Materials: GaN, AlN, InN, BN, SiC, SiGe*, John Wiley & Sons, New York, 2001, p. 31.
- [2] Q. Zhu, W.H. Jiang, K.J. Yatsui, *Appl. Phys.* 86 (1999) 5279.
- [3] H. Kitagawa, Y. Shibutani, S. Ogata, *Modell. Simul. Mater. Sci. Eng.* 3 (1995) 521.
- [4] L.L. Spina, E. Lbona, H. Schellevis, M. Clement, J. Olivares, *Solid-State Electron.* 52 (2008) 1359.
- [5] A.B. Djurisić, N.K. Bundaleski, E.H. Li, *Semicond. Sci. Technol.* 16 (2001) 91.
- [6] L.H. Shen, T. Cheng, L.J. Wu, X.F. Cui, *J. Alloys Compd.* 465 (2008) 562.
- [7] M. Yu, X. Hao, D. Cui, Q. Wang, X. Xu, M. Jiang, *Nanotechnology* 14 (2003) 29.
- [8] G.U. Hu, W. Li, M. Hu, Patent Number CN1893265-A (2007).
- [9] C. Xu, L. Xue, C. Yin, G. Yang, *Phys. Status Solidi A* 198 (2003) 329.
- [10] Q. Wu, Z. Hu, X. Wang, Y. Lu, K. Huo, S. Deng, N. Xu, B. Shen, R. Zhang, Y. Chen, *J. Mater. Chem.* 13 (2003) 2024.
- [11] T. Xie, M. Ye, X.S. Fang, *J. Mater. Technol.* 24 (2008) 608.
- [12] Q. Wu, Z. Hu, X. Wang, Y. Lu, X. Chen, H. Xu, Y. Chen, *J. Am. Chem. Soc.* 125 (2003) 10176.
- [13] Q. Zhao, H.Z. Zhang, X. Xu, Z. Wang, J. Xu, D.P. Yu, G.H. Li, F.H. Su, *Appl. Phys. Lett.* 86 (2005) 193101.
- [14] Q. Wu, Z. Hu, X. Wang, Y. Hu, Y. Tian, Y. Chen, *Diamond Relat. Mater.* 13 (2004) 38.
- [15] H.M. Kim, D.S. Kim, Y.S. Park, D.Y. Kim, T.W. Kang, K.S. Chung, *Adv. Mater. (Weinheim, Ger.)* 14 (2002) 991.
- [16] Y. Kinemuchi, S. Channarong, H. Suematsu, T. Suzuki, W. Jiang, *Pulsed Power Plasma Sci. IEEE Conf. Rec.* 17–22 (2001) 558.
- [17] L. Contursi, G. Bezzi, G. Beghelli, S.P.A. Temav, EP0481563 (April 22) (1992).
- [18] Z.A. Munir, J.B. Holt, *J. Mater. Sci.* 22 (1987) 710.
- [19] L. Yin, Y. Bando, D. Golberg, M. Li, *Adv. Mater. (Weinheim, Ger.)* 16 (2004) 1833.
- [20] B. Schwenzer, L. Loeffler, R. Seshadri, S. Keller, F.F. Lange, S.P. Denbaars, U.K. Mishra, *J. Mater. Chem.* 14 (2004) 637.
- [21] Huimin Lv, Guande Chen, Honggang Ye, Guojun Yan, *J. Appl. Phys.* 101 (2007) 053526.
- [22] M. Remškar, *Adv. Mater. (Weinheim, Ger.)* 16 (2004) 1497.
- [23] S. Luo, W. Zhou, W. Wang, *Appl. Phys. Lett.* 87 (2005) 063109.
- [24] K. Sardar, F.L. Deepak, A. Govindaraj, M.M. Seikh, C.N.R. Rao, *Small* 1 (2005) 91.
- [25] J.A. Dean, *Lange's Handbook of Chemistry*, 13th ed., Mc Graw-Hill, New York, 1985.
- [26] H.T. Chen, X.L. Wu, X. Xiong, *J. Phys. D: Appl. Phys.* 41 (2008) 025101.
- [27] Q. Zhao, H.Z. Zhang, X. Xu, Z. Wang, J. Xu, D.P. Yu, *Appl. Phys. Lett.* 86 (2005) 193101.
- [28] C.Z. Wu, Q. Yang, C. Huang, *J. Solid State Chem.* 177 (2004) 3522.